Nucleon momentum distribution in colliding nuclei and potential between excited nuclei studied with the Vlasov equation

A. Ohnishi and H. Horiuchi
Department of Physics, Kyoto University, Kyoto 606, Japan

T. Wada*
Research Institute for Fundamental Physics, Kyoto University, Kyoto 606, Japan
(Received 13 June 1989)

The momentum distribution of nucleons in colliding $^{16}O+^{16}O$ system is studied with the Vlasov equation in the incident energy region of 20–100 MeV/nucleon. A shift of the momentum distribution to higher momenta is observed until the time of full overlap of two nuclei. It is attributed to the acceleration of the colliding nuclei, and discussed in terms of the newly defined potentials acting between two excited nuclei. The acceleration of colliding excited nuclei is even larger than that in the elastic channel at 40–100 MeV/nucleon. This is due to the dynamical change of the density distribution avoiding high density.

I. INTRODUCTION

The momentum distribution of nucleons in colliding nuclei is an important quantity in the intermediate-energy heavy-ion collision, for instance, for the study of the high-energy particle emission such as the hard photon production. To calculate the momentum distribution in colliding nuclei, we need a specific theory that is microscopic and is able to include excitation of nuclei. The time-dependent Hartree-Fock (TDHF) method and the Vlasov equation[1–3] which is the classical limit of the TDHF are the candidates of such theories and succeeded at low energies. In the intermediate-energy region where the effect of the residual interaction or the two-body collisions becomes important as the incident energy increases, the extended version of the TDHF and the Vlasov-Uehling-Uhlenbeck (VUU) equation[2,3] become more adequate.

Although these theories are one-body theories, namely, they describe the time evolution of the one-body density matrix or the one-body phase-space distribution function, we consider that it is important to investigate the results by these theories from the viewpoint of the nucleus-nucleus relative motion in the intermediate-energy heavy-ion collisions. For example, in the initial stage of the collision, if the energy does not dissipate strongly, it seems to be plausible to expect that the attractive inter-nucleus potential causes the shift of the momentum distribution to the higher momentum side.[4] However this problem, namely, the effect of the nucleus-nucleus interaction on the momentum distribution, has not been so much investigated previously.

In this paper we report the results of the study with the Vlasov equation of the momentum distribution of the $^{16}O+^{16}O$ system in the incident energy region of 20–100 MeV/nucleon.

For this study we have introduced a new definition of the potential between two colliding excited nuclei. In order to define the nucleus-nucleus relative motion, we have to define the center of each nucleus. The use of the test particle method in solving the Vlasov equation gives us one definition to define the center of each nucleus. Namely, we can define the excited nucleus A by the aggregate of the test particles which originally belonged to the nucleus A, and the center of mass of these test particles gives the center of nucleus A. This definition is meaningful when the number of exchanged test particles are not so large. We will see later in this paper that this condition is satisfied even in the strongly overlapping region.

This definition to separate two nuclei gives us the canonically conjugate relative coordinate and momentum $\{\mathbf{R},\mathbf{P}\}$. By the use of these canonical conjugates, it is reasonable to consider that the acceleration of colliding nuclei can be estimated by the potential $\hat{V}$ defined as follows:

$$E=\frac{\mathbf{P}^2}{2\mu}+\hat{V}\ . \tag{1.1}$$

This calculation procedure to get the acceleration potential $\hat{V}$ is analogous to the canonical moving wave-packet method,[5,6] which gives the nucleus-nucleus potential in the elastic channel. Whether the acceleration of colliding excited nuclei is larger than that in the elastic channel or not is not a trivial problem. The dynamical change of density distribution works to lower the potential energy and increases the acceleration, while the excitation of the colliding nuclei results in the energy loss of the nucleus-nucleus relative motion and decreases the acceleration. In our calculation, for relatively high energies $E_{\rm inc}=40$ and 100 MeV/nucleon, the acceleration is even larger than that in the elastic channel, and this large acceleration is expected to increase the high-energy particle production cross section.

When the two-body collisions are turned on, we cannot define the canonical conjugates in a straightforward way,

because the path of each test particle loses sense due to the two-body collisions. So our definition of the potential between colliding nuclei is possible for the Vlasov equation but not for the VUU equation. However, in the low-energy region where the effects of two-body collisions are not so large, it is expected that the main features in the Vlasov dynamics remain and that studying the momentum distribution of colliding nuclei from the viewpoint of nucleus-nucleus relative motion will be a useful tool to understand the VUU analyses of nuclear dynamics. In order to confirm explicitly that this expectation is reasonable, we will show in Sec. VII an example of the comparison between the solutions of the Vlasov and the VUU equations at the incident energy $E_{\rm inc}=20$ MeV/nucleon.

This paper is organized as follows. In Sec. II, the Vlasov equation and the test particle method are reviewed briefly, and the utility of the Gaussian packet which represents a test particle is discussed in Appendix A. In Sec. III, nucleon momentum distributions in the colliding $^{16}O+^{16}O$ system are shown and we introduce a new definition to identify two excited nuclei even in the situation of the strong overlap of the two nuclei. In Sec. IV, the acceleration of the colliding nuclei is estimated. We compare the acceleration in the Vlasov dynamics and that in the elastic channel calculated by the use of canonical moving wave packet. In Sec. V, we calculate the potential between excited nuclei, and discuss the origin of the large acceleration. In Sec. VI, we give an energy dissipation formula. Finally in Sec. VII summary and discussion are given.

II. VLASOV EQUATION AND TEST PARTICLE METHOD

The Vlasov equation, which is obtained by carrying out the Wigner transformation from the TDHF equation and taking the limit $\hbar\to 0$, is written as follows:

$$\frac{Df}{Dt}=\frac{\partial f}{\partial t}+\frac{\mathbf{p}}{m}\cdot\frac{\partial f}{\partial \mathbf{r}}-\frac{\partial U}{\partial \mathbf{r}}\cdot\frac{\partial f}{\partial \mathbf{p}}=0\ . \tag{2.1}$$

Here $f(\mathbf{r},\mathbf{p})$ is the Wigner phase-space distribution function, and $U(\mathbf{r})$ is the mean-field potential which is the Wigner transform of the Hartree-Fock potential. Df/Dt means the increasing rate of the distribution function along the classical path, determined by the Newton equation,

$$\frac{d\mathbf{r}}{dt}=\frac{\mathbf{p}}{m},\quad \frac{d\mathbf{p}}{dt}=-\frac{\partial U}{\partial \mathbf{r}}\ . \tag{2.2}$$

Equation (2.1) means that $f(\mathbf{r},\mathbf{p})$ is constant along the classical path—the classical Liouville's theorem. Pauli's exclusion principle corresponds to $f(\mathbf{r},\mathbf{p})\le g$ (g is spin-isospin degeneracy) in the Vlasov dynamics, and if this condition is satisfied at the initial time, the Pauli principle will not be violated at later time due to the Liouville's theorem.

The effective nuclear force we used is a modified version of the Skyrme VII force or the Bonche, Koonin, and Negele (BKN) force.[7,8] Its two-body part and density-dependent part are given by

$$V_2(\mathbf{r}_1-\mathbf{r}_2)=V_2[(1-M)-MP_\sigma P_\tau]\exp\left[-\frac{(\mathbf{r}_1-\mathbf{r}_2)^2}{\mu^2}\right],$$
$$V_{DD}(\mathbf{r}_1-\mathbf{r}_2)=\frac{t_3}{6}(1+P_\sigma)[\rho(\mathbf{r}_1)]^\sigma\delta(\mathbf{r}_1-\mathbf{r}_2)\ , \tag{2.3}$$

with $V_2=-624.46$ MeV, $M=0.2$, $\mu=0.6791$ fm, and $t_3=17270$ MeV fm^6, $\sigma=1$, respectively. This force is constructed such that the nuclear matter properties are the same as in the case of the Skyrme VII force; namely, at the saturation point, $E/A=-15.77$ MeV, $k_F=1.29$ fm^{-1}, and the incompressibility $K=368$ MeV. For the ^{16}O nucleus, this force gives a binding energy of -135.62 MeV and a root mean square (rms) radius of 2.63 fm for the double closed-shell configuration of the harmonic oscillator bases with the size parameter $\nu=m\omega/2\hbar=0.1623$ fm^{-2}. From this effective force, we get the mean-field potential as follows:

$$U(\mathbf{r})=\int d^3r' v(\mathbf{r}-\mathbf{r}')\rho(\mathbf{r}')+\beta[\rho(\mathbf{r})]^{\sigma+1}\ ,$$
$$\rho(\mathbf{r})=\int\frac{d^3p}{(2\pi\hbar)^3}f(\mathbf{r},\mathbf{p})\ ,$$
$$v(\mathbf{r}-\mathbf{r}')=\tfrac{3}{4}V_2\exp\left[-\frac{(\mathbf{r}-\mathbf{r}')^2}{\mu^2}\right], \tag{2.4}$$
$$\beta=\frac{\sigma+2}{16}t_3\ .$$

It is to be noticed that the Majorana exchange mixture $M=0.2$ makes the exchange contribution vanish and the mean field does not depend on momentum.

The Vlasov equation was solved by the test particle method[1-3] by assigning to each test particle a Gaussian packet with the spatial and momentum spread $\Delta r=0.5$ fm and $\Delta p/\hbar=0.15$ fm^{-1}, respectively. Namely, the distribution function $f(\mathbf{r},\mathbf{p})$ which satisfies the Vlasov equation is obtained by discretizing it by the test particles and solving the classical paths of them. The distribution function $f(\mathbf{r},\mathbf{p})$, and the density $\rho(\mathbf{r})$ are discretized as follows,

$$f(\mathbf{r},\mathbf{p})=\frac{1}{N_0}\sum_{i=1}^{32N_0}d(\mathbf{r}-\mathbf{r}_i,\ \mathbf{p}-\mathbf{p}_i)\ ,$$
$$\rho(\mathbf{r})=\frac{1}{N_0}\sum_{i=1}^{32N_0}d_\rho(\mathbf{r}-\mathbf{r}_i)\ . \tag{2.5}$$

Here $d(\mathbf{r},\mathbf{p})$ and $d_\rho(\mathbf{r})$ are the Gaussian packet and the spatial Gaussian, respectively,

$$d(\mathbf{r},\mathbf{p})=\left[\frac{\hbar}{\Delta r\Delta p}\right]^3\exp\left\{-\frac{1}{2}\left[\left[\frac{\mathbf{r}}{\Delta r}\right]^2+\left[\frac{\mathbf{p}}{\Delta p}\right]^2\right]\right\},$$
$$d_\rho(\mathbf{r})=\left[\frac{1}{\sqrt{2\pi}\Delta r}\right]^3\exp\left[-\frac{1}{2}\left[\frac{\mathbf{r}}{\Delta r}\right]^2\right], \tag{2.6}$$

and N_0 is the test particle number per nucleon. The classical paths of test particles are determined by Newton's equations with a modified mean field $\tilde{U}$,

$$\frac{d\mathbf{r}_i}{dt}=\frac{\mathbf{p}_i}{m},\quad \frac{d\mathbf{p}_i}{dt}=-\left.\frac{\partial \tilde{U}}{\partial \mathbf{r}}\right|_{\mathbf{r}_i}. \tag{2.7}$$

The need to replace U in Eq. (2.2) by $\tilde{U}$ comes from the fact that the Wigner function f was discretized by the Gaussians to get a smooth density and an appropriate mean field. The explicit form of $\tilde{U}$ is shown in Appendix A.

For the initial condition of a single ^{16}O nucleus, the Thomas-Fermi distribution was solved self-consistently, and the phase-space coordinates of test particles were determined by the Monte Carlo method. The Thomas-Fermi distribution $\rho(r)$ of a single ^{16}O is shown in Fig. 1. This distribution gives the binding energy -115 MeV and the rms radius 2.63 fm. The spatial spread $\Delta r=0.5$ fm was chosen as to reproduce the rms radius of the harmonic oscillator closed-shell configuration with $\nu=0.1623$ fm^{-2}, the density distribution of which is also shown in Fig. 1. The number of the test particles per nucleon N_0 was chosen to be 50. We have checked that the results did not change appreciably when N_0 was chosen to be 100.

III. MOMENTUM DISTRIBUTION

Figure 2 shows the time evolution of the momentum distribution $g(k_z)$ in the colliding ^{16}O+^{16}O system at incident energies $E_{\rm inc}=20$, 40, and 100 MeV/nucleon.

$$g(k_z)\equiv\frac{1}{2\pi}\int\frac{d^3r\,dp_x dp_y}{(2\pi\hbar)^2}f(\mathbf{r},\mathbf{p}),\quad k_z=\frac{p_z}{\hbar}. \tag{3.1}$$

Only head-on collisions are treated and k_z is the z component of the single nucleon wave number where z axis is along the beam direction. The time evolution is displayed at three times of which, the first is before the contact of nuclei, the second is at the complete overlap, and the last is after the full overlap. For the sake of convenience we show in Fig. 3 the density distribution $\rho(z)$

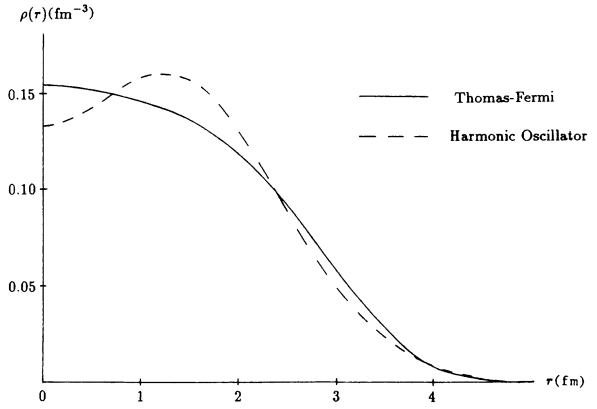

FIG. 1. Thomas-Fermi density distribution $\rho(r)$ of single ^{16}O (solid line). Density distribution of the harmonic oscillator closed-shell configuration with $\nu=0.1623$ fm^{-2} (dashed line) is also shown for comparison. Both of these distributions give the root-mean-square radius $\sqrt{\langle r^2\rangle}=2.63$ fm.

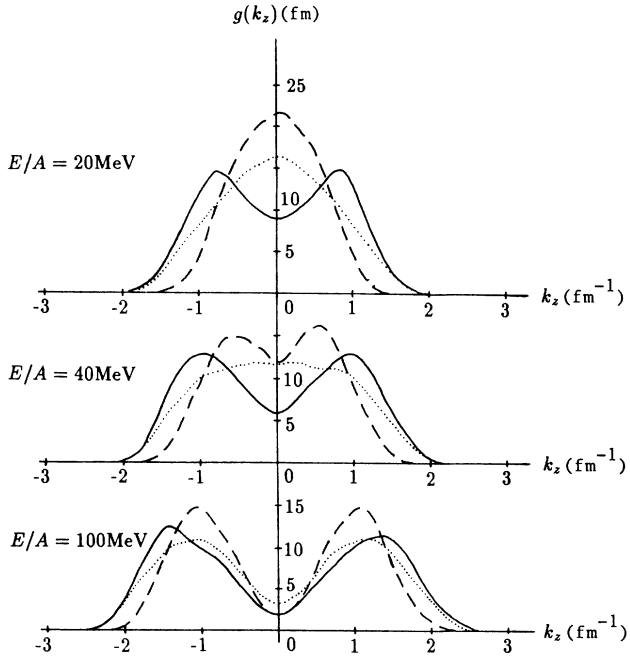

FIG. 2. Time evolution of the nucleon momentum distribution $g(k_z)$ of colliding ^{16}O+^{16}O system for incident energies $E_{\rm inc}=20$, 40, and 100 MeV/nucleon. The dotted, solid, and dashed lines show $g(k_z)$ at the initial time, at the complete overlap and after the full overlap, respectively. The times for the dotted, solid, dashed lines are 0, 40, 80 fm/c for $E_{\rm inc}=20$ MeV/nucleon; 0, 28, 56 fm/c for $E_{\rm inc}=40$ MeV/nucleon; 0, 18, 36 fm/c for $E_{\rm inc}=100$ MeV/nucleon, respectively. Shift to the higher momentum side at the time of the complete overlap is clearly seen.

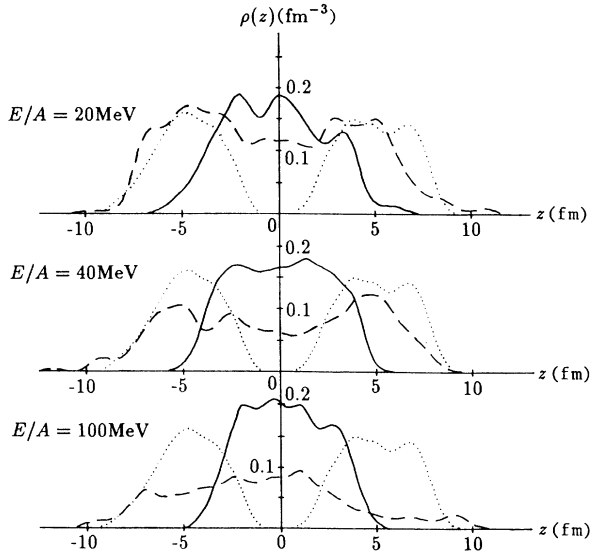

FIG. 3. Time evolution of the nucleon density distribution $\rho(z)$ of colliding ^{16}O+^{16}O system. The incident energies and the time steps are the same as in Fig. 2. The fluctuations are due to the Monte Carlo sampling of the initial condition.

$[=\rho(x=y=0,z)]$ at the same three times. The number of the test particles which build up the density $\rho_1 \sim 0.15$ fm^{-3} can be estimated as

$$n_1 = \frac{N_0 \rho_1}{\langle d_\rho \rangle} \sim 30, \quad \langle d_\rho \rangle = \frac{1}{2(\sqrt{2\pi}\Delta r)^3}, \tag{3.2}$$

where $\langle d_\rho \rangle$ expresses the mean value of the density which is contributed by a single test particle [see Eqs. (2.5) and (2.6)]. From this number, the density fluctuation is about $1/\sqrt{n_1} \sim 0.18$, and the fluctuation in Fig. 3 is in this range.

We note two characteristic features of $g(k_z)$ in Fig. 2. The first is that $g(k_z)$ at the full overlap time has an appreciably increased high-momentum component, if compared to $g(k_z)$ before the contact of nuclei. The second is the appearance of the so-called Pauli pocket[9,10] after the contact of nuclei, which means the depression of $g(k_z)$ around $k_z=0$. The study of the first characteristic is the aim of this paper.

In the case of the Vlasov equation, the use of the test particle method for its solution allows us to identify at any time to which nucleus each test particle originally belonged. Therefore, by grouping all such test particles which originally belonged to one nucleus A, we can define at any time the nucleus A which has suffered excitation because of the collision with the other nucleus. This definition of the excited nucleus may lose its meaning long after the collision on account of the occurrence of the (many) nucleon transfer. However, if used at least before the maximum overlap time of nuclei, this definition, we consider, gives us quite useful information on nuclear dynamics. On the other hand, if we defined the excited nucleus A by the aggregate of test particles which locate spatially on the same side as the original nucleus A with respect to the center of mass, we would meet a difficulty that this excited nucleus A would not be able to reach the other side spatial region with respect to the center of mass by passing through the other nucleus B.

The distribution function of a nucleus α ($=A$ or B) is given by

$$f_\alpha(\mathbf{r},\mathbf{p}) = \frac{1}{N_0} \sum_{i \in \alpha} d(\mathbf{r}-\mathbf{r}_i, \ \mathbf{p}-\mathbf{p}_i), \tag{3.3}$$

and satisfies within the approximation of test particles,

$$\frac{Df_\alpha}{Dt} = \frac{\partial f_\alpha}{\partial t} + \frac{\mathbf{p}}{m} \cdot \frac{\partial f_\alpha}{\partial \mathbf{r}} - \frac{\partial U}{\partial \mathbf{r}} \cdot \frac{\partial f_\alpha}{\partial \mathbf{p}} = 0. \tag{3.4}$$

In Fig. 4 we show the momentum distribution $g_A(k_z)$ of the nucleons belonging to one ^{16}O nucleus A defined in the above-mentioned way. Of course there holds $g(k_z)=g_A(k_z)+g_B(k_z)$. The comparison of Figs. 2 and 4 shows clearly that the $k_z>0$ part of $g(k_z)$ is almost exactly the same as $g_A(k_z)$ except the region $k_z \approx 0$ at the time steps even after full overlap of nuclei. This indicates undoubtedly that our definition of the excited nucleus is very adequate and useful even after the full overlap of nuclei.

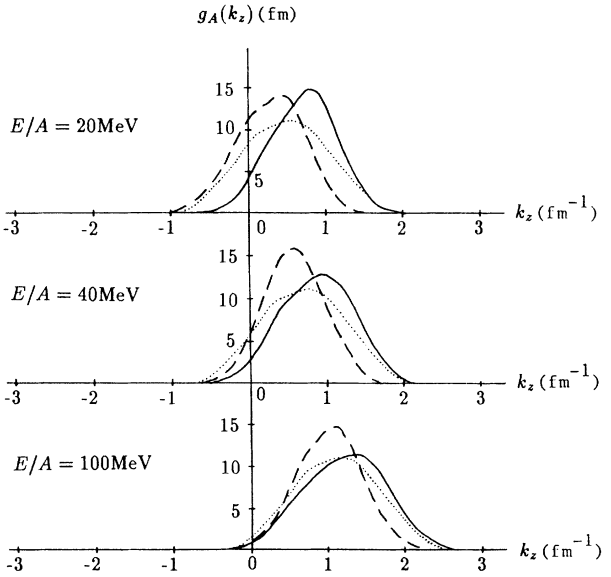

FIG. 4. Time evolution of the nucleon momentum distribution of the "single nucleus A" $g_A(k_z)$ of the colliding ^{16}O+^{16}O system. The incident energies and the time steps are the same as in Fig. 2. At the higher momentum side, $g_A(k_z)$ is almost exactly the same as $g(k_z)$. This means that the transferred nucleons have rather low momenta.

IV. ACCELERATION OF COLLIDING NUCLEI

The increase of the high momentum component of $g_A(k_z)$ or even the shift of $g_A(k_z)$ to higher momentum side at the full overlap time of nuclei will be naturally attributed to the acceleration of colliding nuclei due to the attractive force between them. Since we have the prescription to classify the test particles belonging to different nuclei, we can calculate the center-of-mass kinetic energies of the individual nuclei, the sum of which is the internucleus relative kinetic energy T_r since the momentum of the total center of mass is zero;

$$\begin{aligned} T_r &= \frac{\mathbf{P}^2}{2\mu} = \frac{\mathbf{P}_A^2}{2N_A m} + \frac{\mathbf{P}_B^2}{2N_B m}, \\ \mathbf{P} &= \frac{N_B \mathbf{P}_A - N_A \mathbf{P}_B}{N_A + N_B}, \\ \mathbf{P}_\alpha &= \int \frac{d^3r d^3p}{(2\pi\hbar)^3} \mathbf{p} f_\alpha(\mathbf{r},\mathbf{p}) = \frac{1}{N_0} \sum_{i \in \alpha} \mathbf{p}_i. \end{aligned} \tag{4.1}$$

Here α means A or B, $\mu = N_A N_B m/(N_A+N_B)$ is the reduced mass, and in the ^{16}O+^{16}O case, $N_A=N_B=16$. The amount of the acceleration is measured by the increase of the relative kinetic energy, $T_r - E$, where E is the initial (or incident) relative kinetic energy.

We show in Fig. 5 the quantity $\hat{V} = E - T_r$ as a function of $R(t)$ instead of the time t. Here $R(t)$ is the relative distance at the time t between the centers of mass of two nuclei, and there of course holds a relation $d\mathbf{R}/dt = \mathbf{P}/\mu$,

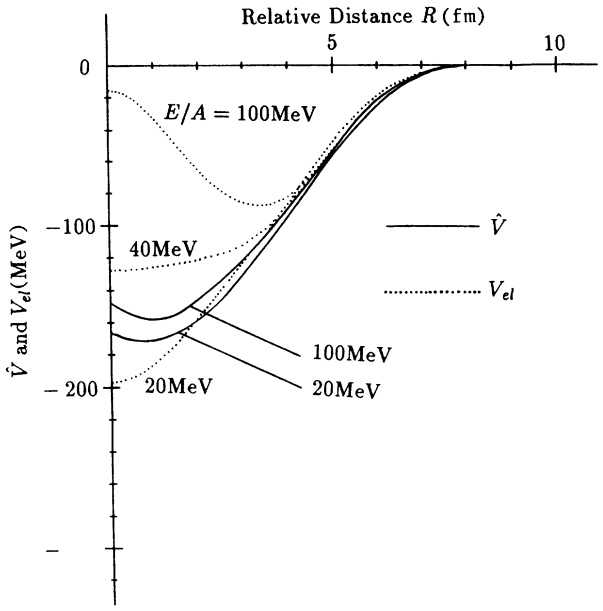

FIG. 5. The acceleration potential energy $\hat{V}=E-T_r$ of the relative motion of the colliding $^{16}O+^{16}O$ system for incident energies $E_{inc}=20$ and 100 MeV/nucleon (solid line). $\hat{V}$ for $E_{inc}=40$ MeV/nucleon is very similar to that for $E_{inc}=20$ MeV/nucleon and so is not shown here. The elastic potential V_{el} calculated by the use of canonical moving wave-packet method is also shown for comparison (dotted line).

$$\mathbf{R}=\mathbf{R}_A-\mathbf{R}_B\ ,$$
$$\mathbf{R}_\alpha=\frac{1}{N_\alpha}\int\frac{d^3r d^3p}{(2\pi\hbar)^3}\mathbf{r}f_\alpha(\mathbf{r},\mathbf{p})=\frac{1}{N_0N_\alpha}\sum_{i\in\alpha}\mathbf{r}_i\ . \tag{4.2}$$

The point $R(t)=0$ corresponds to the full overlap of nuclei. In Fig. 5 only the collision process until the full overlap of two nuclei is analyzed. For comparison, we have also displayed in this figure the potential energy $V_{el}(R)$ of the $^{16}O+^{16}O$ elastic channel which is calculated by the use of the canonical moving wave-packet method[5,6] adopting the same nuclear force. Needless to say $-V_{el}(R)$ expresses the increase of the relative kinetic energy at the internucleus distance R in the elastic channel.

From Fig. 5 we see the potential $\hat{V}$ is almost the same as V_{el} at the tail region. This is very natural because for the tail region we can ignore the excitation of the colliding nuclei and the potential $\hat{V}$ becomes the usual double-folded potential, as V_{el} does. When the overlap of nuclei is large, we see the acceleration of the nuclei is nearly equal to that in the elastic channel for $E_{inc}=20$ MeV/nucleon, and even larger for $E_{inc}=40$ and 100 MeV/nucleon. This point is discussed later in Sec. V.

At the time of the full overlap of nuclei, the depth of $\hat{V}$ which is about -160 MeV means the acceleration is about 20 MeV/nucleon. If we simply convert this amount of acceleration into the shift of the momentum distribution to higher momentum side, the amount of the shift is about 0.20, 0.16, and 0.10 fm^{-1} for $E_{inc}=20$, 40, and 100 MeV/nucleon, respectively. In Fig. 4 we see that the shift of the peak points of the momentum distributions are approximately 0.29, 0.26, and 0.21 fm^{-1} for $E_{inc}=20$, 40, and 100 MeV/nucleon, respectively. Although in Fig. 4 the momentum distributions at the full overlap time of nuclei are not simply obtained by shifting the initial momentum distributions, we can say that the correspondence between $\hat{V}$ of Fig. 5 and time evolution of the momentum distribution in Fig. 4 (or Fig. 2) is good.

V. POTENTIAL BETWEEN EXCITED NUCLEI

Due to the energy conservation, the quantity $\hat{V}(=E-T_r)$ can be expressed as the sum of the excitation energies $(\Delta\epsilon_A+\Delta\epsilon_B)$ of two nuclei and the potential energy V between two excited nuclei;

$$E=T_r+\hat{V}=T_r+V+\Delta\epsilon_A+\Delta\epsilon_B\ . \tag{5.1}$$

The excitation energy of the nucleus α is the increase of the internal energy,

$$\Delta\epsilon_\alpha=\epsilon_\alpha(t)-\epsilon_\alpha(t=-\infty)\ ,$$
$$\epsilon_\alpha=\int\frac{d^3r d^3p}{(2\pi\hbar)^3}\frac{\mathbf{p}^2}{2m}f_\alpha(\mathbf{r},\mathbf{p})-\frac{\mathbf{P}_\alpha^2}{2N_\alpha m}$$
$$+\tfrac{1}{2}\int d^3r d^3r'\rho_\alpha(\mathbf{r})v(\mathbf{r}-\mathbf{r}')\rho_\alpha(\mathbf{r}')$$
$$+\frac{\beta}{2+\sigma}\int d^3r[\rho_\alpha(\mathbf{r})]^{2+\sigma}\ ,$$
$$\rho_\alpha(\mathbf{r})=\int\frac{d^3p}{(2\pi\hbar)^3}f_\alpha(\mathbf{r},\mathbf{p})=\frac{1}{N_0}\sum_{i\in\alpha}d_\rho(\mathbf{r}-\mathbf{r}_i)\ ,$$
$$(\alpha=A\text{ or }B)\ . \tag{5.2}$$

The explicit form of V can be written as

$$V=\int d^3r d^3r'\rho_A(\mathbf{r})v(\mathbf{r}-\mathbf{r}')\rho_B(\mathbf{r}')$$
$$+\frac{\beta}{2+\sigma}\int d^3r\{[\rho(\mathbf{r})]^{2+\sigma}-[\rho_A(\mathbf{r})]^{2+\sigma}$$
$$-[\rho_B(\mathbf{r})]^{2+\sigma}\}\ . \tag{5.3}$$

In the case of $\sigma=1$, this form reduces to the usual double-folding potential;

$$V=\int d^3r d^3r'\rho_A(\mathbf{r})\rho_B(\mathbf{r}')[v(\mathbf{r}-\mathbf{r}')+\beta\rho(\mathbf{r})\delta(\mathbf{r}-\mathbf{r}')]\ . \tag{5.4}$$

The absence of the exchange potential here is of course due to our choice of effective nuclear force with Majorana mixture $M=0.2$. In Fig. 6 we show the potential V as a function of $R(t)$ instead of the time t, like in Fig. 5.

An important property of V is shown in the following relation stating that V gives the driving force of the relative motion,

$$\frac{d\mathbf{P}}{dt}=-\frac{\partial V}{\partial\mathbf{R}}\ ,$$
$$\frac{\partial}{\partial\mathbf{R}}=\frac{N_B}{N_A+N_B}\sum_{i\in A}\frac{\partial}{\partial\mathbf{r}_i}-\frac{N_A}{N_A+N_B}\sum_{i\in B}\frac{\partial}{\partial\mathbf{r}_i}\ , \tag{5.5}$$

a proof of which is presented in Appendix B. Equation (5.5) does not result in the conservation of the quantity

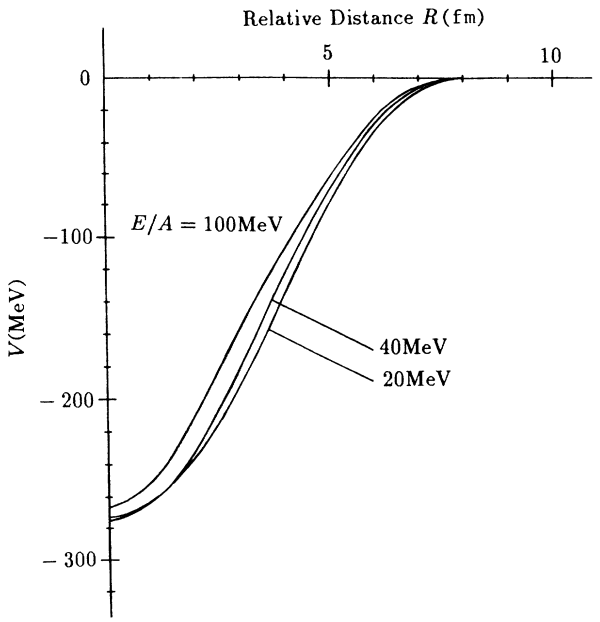

FIG. 6. The potential energy V between two excited ^{16}O nuclei for incident energies $E_{\rm inc}=20$, 40, and 100 MeV/nucleon.

T_r+V. This is because the dependence of V on $\mathbf{r}_i$ is not only through $\mathbf{R}$ (which is a special linear combination of $\mathbf{r}_i$'s [see Eq. (4.2)]) and hence the time dependence of V is not only through $\mathbf{R}$.

The reason why the acceleration in the Vlasov dynamics is even larger than that in the elastic channel in the relatively high-energy region (40 and 100 MeV/nucleon), may be due to the (time-dependent) change of the densities of nuclei which avoid becoming so high as in the elastic channel. In the treatment of the elastic channel by the use of the canonical moving wave-packet method, although the Pauli principle has, in the low-scattering energy region, an effect to make the density of the system lower than the simple sum of the densities of two nuclei, the restriction to keep the nuclei in their ground states makes the density of the system necessarily high especially as the scattering energy gets higher. Due to the density dependence of this stiff nuclear force, a high nuclear density gives us a less attractive potential between nuclei. On the other hand, in the present Vlasov equation, by exciting the colliding nuclei, the system can avoid getting the density high, and thus we get the deeply attractive potential between the excited nuclei. This deeply attractive potential V makes the acceleration potential $\hat{V}$ deep. Figure 3 indeed shows that the density of the system actually avoids becoming high. The maximal density at the full overlap time is at most 0.21 fm^{-3} even at $E=100$ MeV/nucleon, while the density in the elastic channel, calculated by the use of the canonical moving wave-packet method, reaches 0.239, 0.256, and 0.298 fm^{-3} at $E=20$, 40, and 100 MeV/nucleon, respectively.

By definition ($V=\hat{V}-\Delta\epsilon_A-\Delta\epsilon_B$), V is always deeper than $\hat{V}$ in Fig. 5. We see from the difference $\hat{V}-V$ that the excitation energy of one ^{16}O nucleus reaches about 55 MeV, namely, about 3.4 MeV per nucleon at the time of full overlap of nuclei even at $E=20$ MeV/nucleon.

Are these large excitation energies reasonable? To check this, we estimated the excitation energy in the asymptotic region ($R\to\infty$) after the collision. Long after the collision, our definition to separate two nuclei is different from the natural definition because some test particles are necessarily exchanged or transferred. So we have to adopt another definition to separate two nuclei after the collision. A natural way to define the total excitation energy of nuclei long after the collision is to adopt the following definition given, for example, in Eq. (6.40) in Ref. 11;

$$E^{\rm int}=E_{\rm tot}-E^{\rm kin}_{\rm coll}\ ,$$
$$E^{\rm kin}_{\rm coll}=\frac{m}{2}\int d^3r\frac{[\mathbf{J}(\mathbf{r})]^2}{\rho(\mathbf{r})}\ , \tag{5.6}$$
$$\mathbf{J}(\mathbf{r})=\int\frac{d^3p}{(2\pi\hbar)^3}\frac{\mathbf{p}}{m}f(\mathbf{r},\mathbf{p})\ .$$

$E^{\rm int}$ can be considered to be the total excitation energy. In our calculation $E^{\rm kin}_{\rm coll}$ is approximated as follows:

$$E^{\rm kin}_{\rm coll}=\int d^3r\frac{m}{2}\rho(\mathbf{r})\langle\mathbf{V}(\mathbf{r})\rangle^2\simeq\frac{1}{N_0}\sum_i\frac{m}{2}\langle\mathbf{V}(\mathbf{r}_i)\rangle^2\ ,$$
$$\langle\mathbf{V}(\mathbf{r})\rangle=\frac{\mathbf{J}(\mathbf{r})}{\rho(\mathbf{r})}\ . \tag{5.7}$$

The results are $E^{\rm int}=86$, 112, and 142 MeV for $E_{\rm inc}=20$, 40, and 100 MeV/nucleon, respectively, in the asymptotic region. These results do not contradict the previous TDHF calculations. For example, in Ref. 12, for the impact parameter $b=4$ fm, $E^{\rm int}$ are calculated to be 149 and 168 MeV for $E_{\rm inc}=24$ and 36 MeV/nucleon, respectively, and in Ref. 13, for the angular momentum $l=0$, $E^{\rm int}=64$ MeV for $E_{\rm inc}=12$ MeV/nucleon.

The large excitation energies at the time of full overlap of the nuclei calculated by the use of our definition are, we consider, partly due to the following reason. The Vlasov equation is a classical equation and lacks the concept of channel. It should be noticed that in the Vlasov dynamics we cannot distinguish the deformation of the phase-space distribution function f according to the antisymmetrization from that to the real excitation. The former occurs even in the elastic channel. Thus the excitation energy calculated with our definition contains the contribution due to the deformation of f caused by the antisymmetrization effect.

VI. ENERGY DISSIPATION

The dissipation of the total (kinetic and potential) energy of the internucleus relative motion which is the flow of the energy from the relative motion to the excitation (or heating) of the colliding nuclei can be analyzed by using the following formula:

$$\frac{d\Delta\epsilon_\alpha}{dt}=\frac{d\epsilon_\alpha}{dt}=\int d^3r[\mathbf{J}_\alpha(\mathbf{r})-\rho_\alpha(\mathbf{r})\mathbf{V}_\alpha]\left[-\frac{\partial U_{\beta\to\alpha}(\mathbf{r})}{\partial\mathbf{r}}\right],$$

$$\mathbf{V}_\alpha=\frac{d\mathbf{R}_\alpha}{dt}=\frac{\mathbf{P}_\alpha}{N_\alpha m},$$

$$\mathbf{J}_\alpha(\mathbf{r})=\int\frac{d^3p}{(2\pi\hbar)^3}\frac{\mathbf{p}}{m}f_\alpha(\mathbf{r},\mathbf{p}),$$

$$U_{\beta\to\alpha}(\mathbf{r})=\int d^3r'v(\mathbf{r}-\mathbf{r}')\rho_\beta(\mathbf{r}')+\beta\{[\rho(\mathbf{r})]^{\sigma+1}-[\rho_\alpha(\mathbf{r})]^{\sigma+1}\},$$

$$(\alpha,\beta)=(A,B)\ \text{or}\ (B,A). \quad (6.1)$$

A proof of this formula is given in Appendix C. $\mathbf{J}_\alpha(\mathbf{r})$ is the nucleon current of the nucleus α and $\rho_\alpha(\mathbf{r})\mathbf{V}_\alpha$ is the collectively (or uniformly) translational part of $\mathbf{J}_\alpha(\mathbf{r})$. If we regard $U_{\beta\to\alpha}(\mathbf{r})$ to be the one-body force generated by the nucleus β, this formula means that the excitation of the nucleus α is due to the one-body force generated by the nucleus β that acts on the nucleonic motion of the nucleus α which is *not collectively translational.* The nucleonic motion which is not collectively translational can include not only the thermal random motion but also the collective motions like vibrations and rotations. Thus Eq. (6.1) presents a quite reasonable formula for calculating the energy dissipation.

Here, however, there is a question whether the interpretation of $U_{\beta\to\alpha}(\mathbf{r})$ is fully acceptable or not as the one-body potential generated by the nucleus β. This question comes from the part of $U_{\beta\to\alpha}(\mathbf{r})$ due to the density-dependent force. For example, in the case of $\sigma=1$, $U_{\beta\to\alpha}(\mathbf{r})$ takes the following form,

$$U_{\beta\to\alpha}(\mathbf{r})=\int d^3r'\{v(\mathbf{r}-\mathbf{r}')+\beta[\rho(\mathbf{r}')+\rho_\alpha(\mathbf{r}')]\delta(\mathbf{r}-\mathbf{r}')\}\times\rho_\beta(\mathbf{r}'), \quad (6.2)$$

which is of the form of the folding potential generated by the nucleus β. But the density which is used in the density-dependent effective nucleon force is not $\rho(\mathbf{r})$ but $\rho(\mathbf{r})+\rho_\alpha(\mathbf{r})$. At present we do not know the meaning of this additional density $\rho_\alpha(\mathbf{r})$.

VII. SUMMARY AND DISCUSSION

In this paper we firstly calculated the momentum distribution of nucleons in the $^{16}O+^{16}O$ colliding system in the framework of the Vlasov equation in the incident energy region of 20–100 MeV/nucleon. We found that, until the full overlap time of the nuclei, the momentum distribution continues to shift to higher momentum side.

In order to analyze this calculated result, we introduced a new prescription to identify two colliding nuclei even in the strongly overlapping situation. This prescription therefore enables us to trace how two nuclei move and change during the collision process. We calculated the kinetic energy of the internucleus relative motion and found that two nuclei are accelerated during the collision process until the time they overlap fully. The acceleration energy is about 160 MeV at the time of the full overlap of the nuclei in the center of mass system for all the incident energies 20–100 MeV/nucleon, and it is consistent roughly in magnitude with the amount of the shift of the momentum distribution to the higher momentum side. We calculated the acceleration energy in the case of the elastic scattering by using the same effective nuclear force in the framework of the canonical moving wave packet, and found that it is at most 200 MeV at the time of the full overlap of the nuclei for $E_{\text{inc}}=20$ MeV/nucleon and that it decreases as E_{inc} gets higher.

Because of energy conservation, the potential V between two excited nuclei is obtained by substracting the relative kinetic energy and the excitation energies from the incident energy. Thus the value of $-V$ is the sum of two terms; the increase (or the accelerated amount) of the relative kinetic energy from its incident value and the excitation energies of two nuclei. In the present case where the density-dependent part of the effective nuclear force is due to the zero-range three-body force with $\sigma=1$, this potential V was found to be expressed just in the form of the double-folding potential. An important property which V possesses is that it actually gives the driving force for the internucleus relative motion; namely, the negative of the gradient of V with respect to the internucleus relative distance vector is equal to the time derivative of the internucleus relative momentum vector. At the full overlap time of the nuclei, since as mentioned above the increased amount of relative kinetic energy is about 160 MeV and the sum of the excitation energies is about 110 MeV, the depth of V is about 270 MeV. The reason why V gets very deep was attributed to the dynamical change of the density of the system in the Vlasov dynamics. Namely, the density of the system for calculating V is fairly lower compared to that in the elastic channel, since the excitation of nuclei works to make the density lower than in the elastic channel. This deep potential V causes the acceleration effect which remains large even for relatively high incident energies.

Finally, we derived a formula which shows that the excitation of each nucleus is due to the force by the one-body potential generated by the other nucleus acting on such nucleonic motion that is not collectively translational.

In discussing the production of hard photons in the intermediate-energy heavy-ion collision, Yabana and Horiuchi assumed that the colliding excited nuclei are accelerated by the internucleus potential which has similar depth as the elastic scattering potential and argued that this acceleration of the internuclear relative motion causes the increase of the high momentum component of the momentum distribution.[4] The present results of our study by the Vlasov equation gives a strong support to their basic assumptions.

The results that the increase of the high momentum component of the momentum distribution is largely due to the acceleration of the internucleus relative motion, suggests strongly that the momentum distribution is largely influenced by the property of the effective nuclear force whether it gives a deep internucleus potential or not. This viewpoint has not been discussed before in selecting the effective nuclear force to be used in the study of the intermediate-energy heavy-ion reaction. The

effective nuclear force we adopted here gives the volume integral per nucleon pair j_V of the $^{16}O+^{16}O$ elastic channel potential to be 267, 263, and 234 MeV fm^3 for $E_{inc}=20$, 40, and 100 MeV/nucleon, respectively, while recent optical model analyses of the $^{16}O+^{12}C$ elastic scattering give j_V to be about 300, 230, and 170 MeV fm^3 for $E_{inc}=20$, 40, and 100 MeV/nucleon, respectively.[14] Thus we consider that at least for $E_{inc}=20$ and 40 MeV/nucleon, the effective nuclear force we adopted is not so much unreasonable, but for $E_{inc}=100$ MeV/nucleon it is too attractive. On the other hand, simplified local Skyrme interaction whose matter property is the same as Skyrme VII,

$$U(\mathbf{r})=\alpha\left[\frac{\rho(\mathbf{r})}{\rho_0}\right]+\beta\left[\frac{\rho(\mathbf{r})}{\rho_0}\right]^{\sigma+1}, \quad \alpha=-119\ \text{MeV},\ \beta=68.2\ \text{MeV},\ \sigma=1\ , \tag{7.1}$$

gives j_V of the $^{16}O+^{16}O$ elastic channel potential to be 179, 176, and 136 MeV fm^3, for $E_{inc}=20$, 40, and 100 MeV/nucleon, respectively, and these values are too small. (This point is discussed in detail in Ref. 15.)

A distinctive character of the effective nuclear force we adopted is that this force does not give rise to the exchange potential in the Hartree-Fock potential whose Wigner transform is the mean-field potential of the Vlasov equation and does not depend on momentum variable. Although this character is quite unsatisfactory in the standard sense of nuclear physics, most studies of the heavy-ion reaction were made by the use of effective nuclear forces with such character. The exchange potential is indispensable when the energy dependence of the mean field makes an important contribution. The very weak energy dependence of j_V of the calculated elastic channel potential discussed above is mainly due to the character of the present effective nuclear force that does not yield the exchange potential. It is one of our future tasks to make similar studies as the present one by using such effective nuclear force which yields proper exchange component of the mean-field potentials.

The density dependence of the effective nuclear force we adopted may be too strong. This force is usually classified to be a stiff force since it gives $K=368$ MeV for the incompressibility of the nuclear matter. As we discussed in Sec. V the potential between excited nuclei depends strongly on the action of the density-dependent term of the effective nuclear force. Thus it is also one of our future tasks to investigate the effect of the stiffness of the effective nuclear force on the dynamical process we studied here.

Our analysis of the dynamical process in this paper largely depends on the newly introduced prescription to identify two colliding nuclei even in the strongly overlapping situation of two nuclei. The introduction of this prescription was made possible thanks to the fact that we can trace the whole trajectory of every test particle in the case of the Vlasov equation. However, when we treat the Vlasov-Uehling-Uhlenbeck (VUU) equation,[2,3] the two-nucleon collision term makes it impossible to trace the identify of a test particle after the collision with another test particle. Therefore we need some new idea in order to extend our prescription to the VUU equation. Even if this extension is difficult, when we analyze the momentum distribution of nucleons in colliding nuclei in the framework of the VUU equation, our present analyses in the framework of the Vlasov equation are well expected to provide us with very important knowledge about nuclear dynamics at least in the relatively low-energy region.

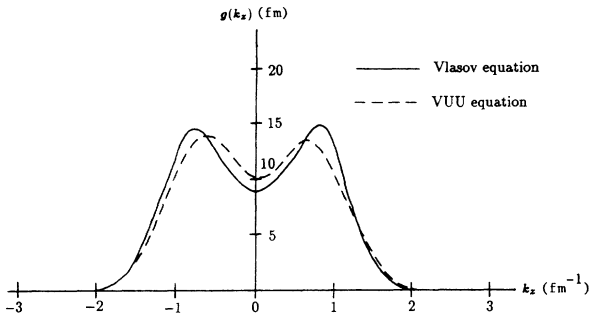

FIG. 7. Comparison between the Vlasov equation and the VUU equation is made by showing the nucleon momentum distributions $g(k_z)$ of the colliding $^{16}O+^{16}O$ system for the incident energy $E_{inc}=20$ MeV/nucleon at the reaction time step $t=40$ fm/c when the two nuclei are completely overlapping. The solid line and the dashed line show the results of the Vlasov equation and the VUU equation, respectively.

To demonstrate this fact, we calculated the momentum distribution by the use of the VUU equation[2] for $^{16}O+^{16}O$ system at the incident energy 20 MeV/nucleon. The result at the time of full overlap of the nuclei is shown in Fig. 7. The momentum distribution calculated with the Vlasov equation at the same reaction time step for the same incident energy is also shown for comparison. The characteristic features of the Vlasov dynamics, the existence of Pauli pocket and the acceleration of the colliding nuclei, are somewhat weakened but clearly seen. This is because two-body collisions are suppressed by the Pauli blocking in the low-energy region. Like this calculation, it is a challenging problem to study the two-body collision effect in the low energy region, namely, to compare the results of the VUU and the Vlasov equation for fusion and deep inelastic collision problems.[16]

ACKNOWLEDGMENTS

The authors thank S. Yamaguchi for his help in numerical work. They also thank Y. Fujiwara and K. Yabana for useful discussions. The computer calculation for this work was supported in part by the Institute for Nuclear Study, University of Tokyo, and Research Center for Nuclear Physics, Osaka University.

APPENDIX A: EQUATION OF MOTION FOR TEST PARTICLES

Test particle with delta function

When the Wigner function is given by the sum of delta functions whose centers satisfy the Newton equation,

$$f(\mathbf{r},\mathbf{p})=\frac{(2\pi\hbar)^3}{N_0}\sum_i \delta(\mathbf{r}-\mathbf{r}_i)\delta(\mathbf{p}-\mathbf{p}_i)\ , \tag{A1}$$

$$\frac{d\mathbf{r}_i}{dt}=\frac{\mathbf{p}_i}{m},\quad \frac{d\mathbf{p}_i}{dt}=-\frac{\partial U}{\partial \mathbf{r}_i}\ , \tag{A2}$$

this Wigner function satisfies the Vlasov equation (2.1) exactly, and if the number of the test particles is infinite, to solve Eq. (A2) is exactly the same as to solve the Vlasov equation because the initial condition of f can be reproduced by Eq. (A1).

Of course, the Vlasov equation (2.1) conserves the total energy:

$$\begin{aligned} E^{\rm tot}&=\int d\tau\frac{\mathbf{p}^2}{2m}f(\mathbf{r},\mathbf{p})+\tfrac{1}{2}\int d^3r\,d^3r'\rho(\mathbf{r})v(\mathbf{r}-\mathbf{r}')\rho(\mathbf{r}')\\ &\quad+\frac{\beta}{2+\sigma}\int d^3r[\rho(\mathbf{r})]^{2+\sigma}=T^{\rm tot}+V^{\rm tot}\ ,\\ d\tau&=\frac{d^3r\,d^3p}{(2\pi\hbar)^3}\ . \end{aligned} \tag{A3}$$

A proof of the energy conservation is as follows. The Vlasov equation (2.1) [and Eq. (A1)] can be written by the use of Poisson bracket (P.B.) with the single-particle Hamiltonian h which is given by the functional derivative of $E^{\rm tot}$,

$$\frac{\partial f}{\partial t}=\{h,f\}_{\rm P.B.}\ ,\quad h=\frac{\delta E^{\rm tot}}{\delta f(\mathbf{r},\mathbf{p})}=\frac{\mathbf{p}^2}{2m}+U(\mathbf{r})\ . \tag{A4}$$

From Eq. (A4), we get the energy conservation formula:

$$\begin{aligned} \frac{dE^{\rm tot}}{dt}&=\int d\tau\frac{\delta E^{\rm tot}}{\delta f}\frac{\partial f}{\partial t}=\int d\tau h\{h,f\}_{\rm P.B.}\\ &=\int d\tau f\{h,h\}_{\rm P.B.}=0\ . \end{aligned} \tag{A5}$$

The replacement $A\{B,C\}_{\rm P.B.}\rightarrow B\{C,A\}_{\rm P.B.}$ in the integration with the phase-space measure $d\tau$ is shown by the integration by parts.

In the numerical calculations, however, in order to get the smooth density distribution and proper mean field we have to treat the Gaussian packet,[3] or it becomes necessary to average them over neighboring cubes in the phase space.[2]

Test particle with the Gaussian packet

If we replace the delta functions in Eq. (A1) with the Gaussian packets as in Eq. (2.5), the resulting distribution function cannot satisfy the Vlasov equation exactly, but it satisfies the Vlasov equation in a *weak sense* if $\mathbf{r}_i$ and $\mathbf{p}_i$ are the solutions of the Newton equation with the Gaussian averaged mean field,

$$\begin{aligned} &\frac{d\mathbf{r}_i}{dt}=\frac{\mathbf{p}_i}{m},\quad \frac{d\mathbf{p}_i}{dt}=-\left.\frac{\partial\langle U\rangle}{\partial\mathbf{r}}\right|_{\mathbf{r}_i},\\ &\langle U\rangle(\mathbf{r})=\int d^3r'd_\rho(\mathbf{r}-\mathbf{r}')U(\mathbf{r}')\ . \end{aligned} \tag{A6}$$

The *weak sense* means that following relations hold:

$$\int d^3r\frac{Dd_i}{Dt}=0,\quad \int d^3p\frac{Dd_i}{Dt}=0\ ,\quad d_i=d(\mathbf{r}-\mathbf{r}_i,\ \mathbf{p}-\mathbf{p}_i)\ . \tag{A7}$$

This is largely due to the fact that the Gaussian packet is the product of F_i and G_i, spatial and momentum Gaussians.

$$d(\mathbf{r}-\mathbf{r}_i,\ \mathbf{p}-\mathbf{p}_i)=F_i\times G_i\ ,$$

$$F_i=d_\rho(\mathbf{r}-\mathbf{r}_i)=\frac{1}{(\sqrt{2\pi}\Delta r)^3}\exp\left[-\frac{(\mathbf{r}-\mathbf{r}_i)^2}{2(\Delta r)^2}\right]\ , \tag{A8}$$

$$G_i=\left[\frac{\sqrt{2\pi}\hbar}{\Delta p}\right]^3\exp\left[-\frac{(\mathbf{p}-\mathbf{p}_i)^2}{2(\Delta p)^2}\right]\ .$$

A proof of this is as follows. Dd_i/Dt becomes

$$\begin{aligned} \frac{Dd_i}{Dt}&=\left[\left[-\frac{d\mathbf{r}_i}{dt}+\frac{\mathbf{p}}{m}\right]\cdot\frac{\partial}{\partial\mathbf{r}}-\left[\frac{d\mathbf{p}_i}{dt}+\frac{\partial U}{\partial\mathbf{r}}\right]\frac{\partial}{\partial\mathbf{p}}\right]d_i\\ &=\left[-\frac{d\mathbf{r}_i}{dt}+\frac{\mathbf{p}}{m}\right]\cdot\frac{\partial F_i}{\partial\mathbf{r}}G_i-\left[\frac{d\mathbf{p}_i}{dt}+\frac{\partial U}{\partial\mathbf{r}}\right]\frac{\partial G_i}{\partial\mathbf{p}}F_i\ . \end{aligned} \tag{A9}$$

When we integrate Eq. (A9) over $\mathbf{r}$, the first term becomes the surface term and vanishes, and the second term becomes

$$\begin{aligned} \int d^3r\frac{Dd_i}{Dt}&=-\frac{\partial G_i}{\partial\mathbf{p}}\cdot\int d^3r\left[\frac{d\mathbf{p}_i}{dt}+\frac{\partial U}{\partial\mathbf{r}}\right]d_\rho(\mathbf{r}-\mathbf{r}_i)\\ &=-\frac{\partial G_i}{\partial\mathbf{p}}\cdot\left[\frac{d\mathbf{p}_i}{dt}+\left.\frac{\partial\langle U\rangle}{\partial\mathbf{r}}\right|_{\mathbf{r}_i}\right]=0\ . \end{aligned} \tag{A10}$$

Simlarly,

$$\begin{aligned} \int d^3p\frac{Dd_i}{Dt}&=\frac{\partial F_i}{\partial\mathbf{r}}\cdot\int d^3p\left[-\frac{d\mathbf{r}_i}{dt}+\frac{\mathbf{p}}{m}\right]G_i\\ &=(2\pi\hbar)^3\frac{\partial F_i}{\partial\mathbf{r}}\cdot\left[-\frac{d\mathbf{r}_i}{dt}+\frac{\mathbf{p}_i}{m}\right]=0\ . \end{aligned} \tag{A11}$$

By the use of Eq. (A7), we get the Vlasov equation in a weak sense:

$$\int d^3r\frac{Df}{Dt}=\int d^3p\frac{Df}{Dt}=0\ , \tag{A12}$$

and the total energy is conserved as in the Eq. (A5) because we can replace $\partial f/\partial t$ by $\{h,f\}_{\rm P.B.}$ in the integral,

$$\begin{aligned} \frac{dE^{\rm tot}}{dt}&=\int d\tau h\frac{\partial f}{\partial t}\\ &=\int\frac{d^3p}{(2\pi\hbar)^3}\frac{\mathbf{p}^2}{2m}\int d^3r\{h,f\}_{\rm P.B.}\\ &\quad+\int\frac{d^3r}{(2\pi\hbar)^3}U(\mathbf{r})\int d^3p\{h,f\}_{\rm P.B.}\\ &=\int d\tau h\{h,f\}_{\rm P.B.}=0\ . \end{aligned} \tag{A13}$$

[Equation (A6) is the same as that of Ref. 3.]

If f is given by Eq. (2.5) and if $\sigma=1$, $E^{\rm tot}$ is written as

$$E^{\rm tot}=T_0+\frac{1}{N_0}\sum_i\frac{\mathbf{p}_i^2}{2m}+\frac{1}{2N_0^2}\sum_{i,j}\bar{v}(\mathbf{r}_i-\mathbf{r}_j)+\frac{\beta}{3N_0^3}\sum_{i,j,k}d_3(\mathbf{r}_i,\mathbf{r}_j,\mathbf{r}_k)\ ,$$
$$T_0=3(N_A+N_B)\times\frac{(\Delta p)^2}{2m}\ ,$$
$$\bar{v}(\mathbf{r}_i-\mathbf{r}_j)=\tfrac{3}{4}V_2\left[\frac{\mu^2}{\mu^2+4(\Delta r)^2}\right]^{3/2}\exp\left[-\frac{(\mathbf{r}_i-\mathbf{r}_j)^2}{\mu^2+4(\Delta r)^2}\right]\ , \tag{A14}$$
$$d_3(\mathbf{r}_i,\mathbf{r}_j,\mathbf{r}_k)=\frac{1}{[2\sqrt{3}\pi(\Delta r)^2]^3}\sum_{i,j,k}\exp\left[-\frac{(\mathbf{r}_i-\mathbf{r}_j)^2+(\mathbf{r}_j-\mathbf{r}_k)^2+(\mathbf{r}_k-\mathbf{r}_i)^2}{6(\Delta r)^2}\right]\ ,$$

and the Gaussian averaged mean field $\langle U\rangle$ is written as

$$\langle U\rangle(\mathbf{r})=\frac{1}{N_0}\sum_i\bar{v}(\mathbf{r}-\mathbf{r}_i)+\frac{\beta}{N_0^2}\sum_{i,j}d_3(\mathbf{r},\mathbf{r}_i,\mathbf{r}_j)\ . \tag{A15}$$

Vlasov equation with the Gaussian modified interaction

We can get Eq. (A6) from another point of view. When the distribution function of test particles $f^{\rm tp}$ is given by the sum of delta functions, and the interaction which test particles feel is averaged by the Gaussian, namely,

$$f^{\rm tp}(\mathbf{r},\mathbf{p})=\frac{(2\pi\hbar)^3}{N_0}\sum_i\delta(\mathbf{r}-\mathbf{r}_i)\delta(\mathbf{p}-\mathbf{p}_i),\quad \rho^{\rm tp}(\mathbf{r})=\frac{1}{N_0}\sum_i\delta(\mathbf{r}-\mathbf{r}_i)\ ,$$
$$V^{\rm tot}=\tfrac{1}{2}\int d^3r d^3r'\rho^{\rm tp}(\mathbf{r})\bar{v}(\mathbf{r}-\mathbf{r}')\rho^{\rm tp}(\mathbf{r}')+\frac{\beta}{2+\sigma}\int d^3r_1d^3r_2d^3r_3\rho^{\rm tp}(\mathbf{r}_1)\rho^{\rm tp}(\mathbf{r}^2)\rho^{\rm tp}(\mathbf{r}^3)\rho^{\rm tp}d_3(\mathbf{r}_1,\mathbf{r}_2,\mathbf{r}_3)\ , \tag{A16}$$

the mean field $\delta V^{\rm tot}/\delta\rho^{\rm tp}$ becomes the same as $\langle U\rangle$, and we get the Vlasov equation with the Gaussian averaged interaction:

$$\frac{\partial f^{\rm tp}}{\partial t}+\frac{\mathbf{p}}{m}\cdot\frac{\partial f^{\rm tp}}{\partial\mathbf{r}}-\frac{\partial\langle U\rangle}{\partial\mathbf{r}}\cdot\frac{\partial f^{\rm tp}}{\partial\mathbf{p}}=0\ . \tag{A17}$$

From this equation we get Eq. (A6) again. In summary the correspondence is as follows:

$$f(\mathbf{r},\mathbf{p})\leftrightarrow f^{\rm tp}(\mathbf{r},\mathbf{p}),\quad U(\mathbf{r})\leftrightarrow\langle U\rangle(\mathbf{r})\ , \tag{A18}$$
$$f(\mathbf{r},\mathbf{p})=\int d\tau' d(\mathbf{r}-\mathbf{r}',\mathbf{p}-\mathbf{p}')f^{\rm tp}(\mathbf{r}',\mathbf{p}')\ . \tag{A19}$$

However, in the actual calculation of Eq. (A6), we have a problem of the computational time. Because of the three-body interaction in Eq. (A6), double-loop sum over all test particles for each test particle is necessary, and the number of the terms to be summed amounts to a few billion for each time step. To avoid this problem, we adopted the following Gaussian modified interaction,

$$V^{\rm tot}=\tfrac{1}{2}\int d^3r\,d^3r'\rho^{\rm tp}(\mathbf{r})\bar{v}(\mathbf{r}-\mathbf{r}')\rho^{\rm tp}(\mathbf{r}')+\frac{\beta}{2+\sigma}\int d^3r_1d^3r_2d^3r_3\rho^{\rm tp}(\mathbf{r}_1)d_\rho(\mathbf{r}_1-\mathbf{r}_2)\rho^{\rm tp}(\mathbf{r}_2)\tilde{d}_\rho(\mathbf{r}_2-\mathbf{r}_3)\rho^{\rm tp}(\mathbf{r}_3)$$
$$=\frac{1}{2N_0^2}\sum_{i,j}\bar{v}(\mathbf{r}_i-\mathbf{r}_j)+\frac{\beta}{3N_0^3}\sum_{i,j,k}d_\rho(\mathbf{r}_i-\mathbf{r}_j)\tilde{d}_\rho(\mathbf{r}_i-\mathbf{r}_k)\ , \tag{A20}$$
$$f^{\rm tp}(\mathbf{r},\mathbf{p})=\frac{(2\pi\hbar)^3}{N_0}\sum_i\delta(\mathbf{r}-\mathbf{r}_i)\delta(\mathbf{p}-\mathbf{p}_i),\quad \rho^{\rm tp}(\mathbf{r})=\frac{1}{N_0}\sum_i\delta(\mathbf{r}-\mathbf{r}_i)\ ,$$

where d_ρ is the spatial Gaussian of test particle [Eq. (2.6)], and $\tilde{d}_\rho(\mathbf{r}_i-\mathbf{r}_j)$ is its Gaussian folding,

$$\tilde{d}_\rho(\mathbf{r}_i-\mathbf{r}_j)=\frac{1}{(\sqrt{4\pi}\Delta r)^3}\exp\left[-\frac{(\mathbf{r}_i-\mathbf{r}_j)^2}{4(\Delta r)^2}\right]=\int d^3r\,d_\rho(\mathbf{r}_i-\mathbf{r})d_\rho(\mathbf{r}-\mathbf{r}_j)\ . \tag{A21}$$

From this Gaussian modified interaction, single-particle Hamiltonian is given as

$$h(\mathbf{r},\mathbf{p})=\frac{\mathbf{p}^2}{2m}+\tilde{U}(\mathbf{r})\ ,$$
$$\tilde{U}=\frac{1}{N_0}\sum_j\bar{v}(\mathbf{r}-\mathbf{r}_j)+\frac{\beta}{3N_0^2}\sum_{j,k}[d_\rho(\mathbf{r}-\mathbf{r}_j)\tilde{d}_\rho(\mathbf{r}-\mathbf{r}_k)+d_\rho(\mathbf{r}_j-\mathbf{r})\tilde{d}_\rho(\mathbf{r}_j-\mathbf{r}_k)+d_\rho(\mathbf{r}_j-\mathbf{r}_k)\tilde{d}_\rho(\mathbf{r}_j-\mathbf{r})]\ , \tag{A22}$$

and the classical paths of test particles are determined by Eq. (2.7):

$$\frac{d\mathbf{r}_i}{dt}=\frac{\mathbf{p}_i}{m},\quad \frac{d\mathbf{p}_i}{dt}=-\left.\frac{\partial\tilde{U}(\mathbf{r})}{\partial\mathbf{r}}\right|_{\mathbf{r}_i}. \tag{2.7}$$

We have checked that Eq. (2.7) is a good approximation of Eq. (A6) in the case of one-dimensional slab-slab collision.

All of our calculations were carried out by Eqs. (A20)–(A22), and Eq. (2.7), and we considered that the distribution function of nucleon is given by Eq. (A19). For example, the Thomas-Fermi distribution was solved self-consistently with $\rho^{\rm tp}$ and $\tilde{U}$, and the nucleon distribution was given by

$$\rho(\mathbf{r})=\int d^3r' d_\rho(\mathbf{r}-\mathbf{r}')\rho^{\rm tp}(\mathbf{r}')\ . \tag{A23}$$

This nucleon distribution function f satisfies Eq. (A11), but Eq. (A10) does not hold. Namely,

$$\int d^3r\frac{Dd_i}{Dt}\neq 0\ ,\quad \int d^3p\frac{Dd_i}{Dt}=0\ . \tag{A24}$$

This is because $\tilde{U}$ cannot be expressed in the form of $\langle U\rangle$.

APPENDIX B: POTENTIAL OF NUCLEUS-NUCLEUS RELATIVE MOTION

From Eqs. (3.4) and (4.2) we get $d\mathbf{R}_\alpha/dt$ as follows:

$$\frac{d\mathbf{R}_\alpha}{dt}=\frac{1}{N_\alpha}\int d\tau\left[-\frac{\mathbf{p}}{m}\cdot\frac{\partial f_\alpha}{\partial\mathbf{r}}+\frac{\partial U}{\partial\mathbf{r}}\cdot\frac{\partial f_\alpha}{\partial\mathbf{p}}\right]\mathbf{r}=\frac{1}{N_\alpha}\int d\tau\frac{\mathbf{p}}{m}f_\alpha=\frac{\mathbf{P}_\alpha}{N_\alpha m}\ . \tag{B1}$$

From this equation we have

$$\frac{d\mathbf{R}}{dt}=\frac{\mathbf{P}_A}{N_A m}-\frac{\mathbf{P}_B}{N_B m}=\frac{\mathbf{P}}{\mu}\ . \tag{B2}$$

Similarly, from Eqs. (3.4) and (4.1) there holds

$$\frac{d\mathbf{P}_\alpha}{dt}=\int d\tau\left[-\frac{\mathbf{p}}{m}\cdot\frac{\partial f_\alpha}{\partial\mathbf{r}}+\frac{\partial U}{\partial\mathbf{r}}\cdot\frac{\partial f_\alpha}{\partial\mathbf{p}}\right]\mathbf{p}=-\int d^3r\rho_\alpha(\mathbf{r})\frac{\partial U(\mathbf{r})}{\partial\mathbf{r}}=\int d^3r\frac{\partial\rho_\alpha(\mathbf{r})}{\partial\mathbf{r}}U(\mathbf{r})\ . \tag{B3}$$

If we define the density from the center of the nucleus α

$$\rho_\alpha^{\rm int}(\mathbf{r}-\mathbf{R}_\alpha)=\rho_\alpha(\mathbf{r})\ , \tag{B4}$$

$\partial/\partial\mathbf{r}$ in Eq. (B3) can be replaced by $\partial/\partial\mathbf{R}_\alpha$:

$$\int d^3r\frac{\partial\rho_\alpha}{\partial\mathbf{r}}U(\mathbf{r})=-\int d^3r\frac{\partial\rho_\alpha^{\rm int}}{\partial\mathbf{R}_\alpha}\frac{\delta V^{\rm tot}}{\delta\rho_\alpha^{\rm int}}=-\frac{\partial V^{\rm tot}}{\partial\mathbf{R}_\alpha}\ . \tag{B5}$$

Recall that the mean field $U(\mathbf{r})$ is given by the functional derivative of $V^{\rm tot}$ with respect to $\rho(\mathbf{r})$:

$$U(\mathbf{r})=\frac{\delta V^{\rm tot}}{\delta\rho(\mathbf{r})}=\frac{\delta V^{\rm tot}}{\delta\rho_\alpha(\mathbf{r})}=\frac{\delta V^{\rm tot}}{\delta\rho_\alpha^{\rm int}(\mathbf{r}-\mathbf{R}_\alpha)}\ . \tag{B6}$$

In $V^{\rm tot}$ the intrinsic potential energy,

$$V_\gamma^{\rm int}=\tfrac{1}{2}\int d^3r\,d^3r'\rho_\gamma(\mathbf{r})v(\mathbf{r}-\mathbf{r}')\rho_\gamma(\mathbf{r}')+\frac{\beta}{\sigma+2}\int d^3r[\rho_\gamma(\mathbf{r})]^{\sigma+2}\quad(\gamma=A\ \text{or}\ B)\ , \tag{B7}$$

does not depend on $\mathbf{R}_\alpha$ and can be subtracted from $V^{\rm tot}$ in Eq. (B5):

$$V=V^{\rm tot}-V_A^{\rm int}-V_B^{\rm int}\ . \tag{B8}$$

From Eqs. (B3) and (B5) we get Eq. (5.4) describing the nucleus-nucleus relative motion:

$$\frac{d\mathbf{P}}{dt}=-\frac{N_B}{N_A+N_B}\frac{\partial V}{\partial\mathbf{R}_A}+\frac{N_A}{N_A+N_B}\frac{\partial V}{\partial\mathbf{R}_B}=-\frac{\partial V}{\partial\mathbf{R}}\ . \tag{B9}$$

Even when we use the test particle method, Eq. (B9) is exact if we solve Eq. (A6), because thanks to Eq. (A7) we can use the Vlasov equation for single nuclei Eq. (3.4) in the integral like in Eq. (A13). When we use Eq. (2.7) instead of Eq. (A6), Eq. (B9) is also exact. In order to prove this we have to replace f by $f^{\rm tp}$ and $V_\alpha^{\rm int}$ of Eq. (B7) by the following:

$$V_\alpha^{\rm int}=\frac{1}{2N_0^2}\sum_{i,j\in\alpha}\tilde{v}(\mathbf{r}_i-\mathbf{r}_j)+\frac{\beta}{3N_0^3}\sum_{i,j,k\in\alpha}d_\rho(\mathbf{r}_i-\mathbf{r}_j)\tilde{d}_\rho(\mathbf{r}_i-\mathbf{r}_k)\ . \tag{B10}$$

APPENDIX C: ONE-BODY ENERGY DISSIPATION IN THE VLASOV EQUATION

The internal energy of nucleus α is written as

$$\epsilon_\alpha = \int d\tau \frac{\mathbf{p}^2}{2m} f_\alpha - \frac{\mathbf{P}_\alpha^2}{2N_\alpha m} + V_\alpha^{\rm int} \ . \tag{C1}$$

To calculate $d\epsilon/dt$, the following formula is useful:

$$\frac{\partial \rho_\alpha(\mathbf{r})}{\partial t} = -\frac{\partial \mathbf{J}_\alpha}{\partial \mathbf{r}} \ , \quad \mathbf{J}_\alpha(\mathbf{r}) = \int \frac{d^3p}{(2\pi\hbar)^3} \frac{\mathbf{p}}{m} f_\alpha(\mathbf{r},\mathbf{p}) \ . \tag{C2}$$

$\partial \mathbf{J}_\alpha/\partial \mathbf{r}$ means the divergence of $\mathbf{J}_\alpha$. Since $\mathbf{J}_\alpha$ means the local current of nucleons belonging to the nucleus α, this is the continuity equation and can be obtained from Eq. (3.3).

By the use of this equation, we get Eq. (6.1),

$$\begin{aligned}
\frac{d\epsilon_\alpha}{dt} &= \int d\tau \frac{\mathbf{p}^2}{2m} \left[\frac{\partial U}{\partial \mathbf{r}} \cdot \frac{\partial f_\alpha}{\partial \mathbf{p}} \right] - \frac{\mathbf{P}_\alpha}{N_\alpha m} \cdot \frac{d\mathbf{P}_\alpha}{dt} - \int d^3r \frac{\partial \mathbf{J}_\alpha}{\partial \mathbf{r}} \frac{\delta V_\alpha^{\rm int}}{\delta \rho_\alpha} \\
&= -\int d\tau \frac{\mathbf{p}}{m} f_\alpha \cdot \frac{\partial U}{\partial \mathbf{r}} - \int d^3r \frac{\partial \mathbf{J}_\alpha}{\partial \mathbf{r}} U_\alpha - \mathbf{V}_\alpha \cdot \frac{d\mathbf{P}_\alpha}{dt} \\
&= -\int d^3r \mathbf{J}_\alpha \cdot \frac{\partial}{\partial \mathbf{r}} [U(\mathbf{r}) - U_\alpha(\mathbf{r})] + \mathbf{V}_\alpha \cdot \int d^3r \rho_\alpha(\mathbf{r}) \frac{\partial U(\mathbf{r})}{\partial \mathbf{r}} \\
&= \int d^3r [\mathbf{J}_\alpha(\mathbf{r}) - \rho_\alpha(\mathbf{r}) \mathbf{V}_\alpha] \cdot \left[-\frac{\partial U_{\beta \to \alpha}(\mathbf{r})}{\partial \mathbf{r}} \right] ,
\end{aligned} \tag{C3}$$

where U_α and $U_{\beta \to \alpha}$ are given by

$$\begin{aligned}
U_\alpha(\mathbf{r}) &= \frac{\delta V_\alpha^{\rm int}}{\delta \rho_\alpha(\mathbf{r})} = \int d^3r' v(\mathbf{r}-\mathbf{r}') \rho_\alpha(\mathbf{r}') + \beta [\rho_\alpha(\mathbf{r})]^{\sigma+1} \ , \\
U_{\beta \to \alpha} &= U(\mathbf{r}) - U_\alpha(\mathbf{r}) \ .
\end{aligned} \tag{C4}$$

Even when we use the test particle method, Eq. (A7) or Eq. (A24) guarantees Eq. (C2) to hold and hence the formulas in this Appendix remain exact.

---

*Present address: The Institute of Physical and Chemical Research (RIKEN), Wako-shi, Japan.

[1]C. Y. Wong, Phys. Rev. C **25**, 1460 (1982).
[2]G. F. Bertsch and S. Das Gupta, Phys. Rep. **160**, 189 (1988).
[3]C. Grégoire, B. Remaud, F. Sébille, L. Vinet, and Y. Raffray, Nucl. Phys. **A465**, 317 (1987).
[4]K. Yabana and H. Horiuchi, J. Phys. Soc. Jpn. Suppl. **58**, 705 (1989); Prog. Theor. Phys. **82**, 86 (1989).
[5]M. Saraceno, P. Kramer, and F. Fernandez, Nucl. Phys. **A405**, 88 (1983).
[6]S. Yamaguchi, K. Yabana, and H. Horiuchi, Prog. Theor. Phys. **82**, 53 (1989).
[7]P. Bonche, S. Koonin, and J. W. Negele, Phys. Rev. C **13**, 1226 (1976).
[8]T. Wada, Master thesis, Kyoto University, 1982 (unpublished).
[9]W. Bauer, G. F. Bertsch, W. Cassing, and U. Mosel, Phys. Rev. C **34**, 2127 (1986).
[10]T. S. Biro, K. Niita, A. L. De Paoli, W. Bauer, W. Cassing, and U. Mosel, Nucl. Phys. **A475**, 579 (1987).
[11]P. Schuck, R. W. Hasse, J. Jaenicke, C. Grégoire, B. Remaud, F. Sébille, and E. Suraud, Prog. Part. Nucl. Phys. **22**, 181 (1989).
[12]R. Y. Cusson, J. A. Maruhn, and H. W. Meldner, Phys. Rev. C **18**, 2589 (1978).
[13]S. E. Koonin, K. T. R. Davies, V. Maruhn-Rezwani, H. Feldmeier, S. J. Krieger, and J. W. Negele, Phys. Rev. C **15**, 1359 (1977).
[14]M.-E. Brandan, Phys. Rev. Lett. **60**, 784 (1988).
[15]T. Wada, S. Yamaguchi, and H. Horiuchi, Phys. Rev. C **41**, 160 (1990).
[16]T. Maruyama, A. Ohnishi, and H. Horiuchi, to be submitted to Phys. Rev. C.